

Crystallinity Effect on the Gas Transport in Semicrystalline Coextruded Films Based on Linear Low Density Polyethylene

VICENTE COMPAÑ,¹ L. F. DEL CASTILLO,² S. I. HERNÁNDEZ,² M. MAR LÓPEZ-GONZÁLEZ,³ EVARISTO RIANDE³

¹Departamento de Termodinámica Aplicada, ETSII, Universidad Politécnica de Valencia, Campus de Vera s/n, 46022-Valencia, Spain

²Departamento de Polímeros, Instituto de Investigaciones en Materiales, Universidad Nacional Autónoma de México, Ciudad Universitaria, Apartado Postal 70-360, Coyoacán, México DF, 04510

³Instituto de Ciencia y Tecnología de Polímeros (CSIC), 28006 Madrid, Spain

Received 11 August 2009; revised 1 December 2009; accepted 9 December 2009

DOI: 10.1002/polb.21932

Published online in Wiley InterScience (www.interscience.wiley.com).

ABSTRACT: This article describes the diffusion and permeability of oxygen, carbon dioxide, methane, ethane, ethylene, propane, and propylene in 1-octene based polyethylene of densities 0.94, 0.92, 0.904, and 0.87. The isotherms obtained in the time-lag experimental device display a diffusion coefficient and permeability behavior similar to that of glassy polymers. We apply the dual model to semicrystalline polymers assuming that Henry's sites are related to the amorphous phase, which decreases when the crystallinity percentage increases. Whereas the interphase of the polymeric matrix and the crystalline phase prevails and acts as Langmuir sites. Their effect is to increase both, the tortuosity of diffusion trajectories and the chain immobilization. We now explain this effect using thermodynamic considerations. In fact, the tortuosity is related to the change in activation

entropy, and the chain immobilization to the cohesive energy of the polymeric matrix. In those terms, the diffusion coefficient does not follow the same crystalline percentage dependence than the solubility. According to the previous findings, the solubility changes in proportion to amorphous percentages. Instead, diffusion coefficient has exponential dependence. Furthermore, we show that the permeability changes as a consequence of the modification of diffusion and solubility, according to the product of both quantities. Comparison with previous publication has been included. © 2010 Wiley Periodicals, Inc. *J Polym Sci Part B: Polym Phys* 48: 634–642, 2010

KEYWORDS: crystallinity; gas diffusion; permeability; polyethylene; solubility; sorption

INTRODUCTION Diffusion or transport of a chemical species of low molecular weight in both rubbery and glass polymers is a topic of interest in many fields of science and technology. Their importance has been growing over the past few years regarding the development of polymer films as separation barriers used for packaging food and beverages, cable covered protection, encapsulating drugs with controlled delivery, elaborating contact lenses, and manufacturing ion-exchange membranes.¹

One of the most promising application of polymers comes in the industry of separation of gas mixtures, such as helium from natural gas, oxygen from nitrogen, as well as hydrogen and methane purification.^{2,3} Most membranes used in the separation of gas mixtures are made from polymeric substances, with high glass transition temperatures, such as polysulfones, polyamides, cellulose triacetate.

The mechanism of gas separation by such membranes is called solution-diffusion, and it consists of three steps: (1) Absorption or adsorption upon the upstream boundary, (2) Activated diffusion through the membrane, and (3) Dissolu-

tion or evaporation from the downstream boundary. The drive force for diffusion is given by the difference in thermodynamic activity established at the upstream and downstream faces of the membrane. In most cases, the gas sorption results proportional to Henry's law and the solubility of the gas in the polymer is linearly dependent to its partial pressure. It should be noted that the gas sorption involves molecular interactions between the gas and the chemical components of the polymer. On the other hand, the diffusion is controlled by the free volume and the intramolecular mobility. The gas permeability is a consequence of both processes expressed as their product.

The development of new gas separation membranes is oriented to obtain a good balance of two properties, namely permeability and permselectivity. To improve these properties, a better knowledge of the relationship between chemical structure, thermodynamics and transport parameters is needed.^{4–8}

Along these lines, the study of films made from Linear PE of Low Density (LLDPE) and relatively low crystalline degree

Correspondence to: V. Compañ (E-mail: vicommo@ter.upv.es)

Journal of Polymer Science: Part B: Polymer Physics, Vol. 48, 634–642 (2010) © 2010 Wiley Periodicals, Inc.

has been reported.⁹ The interest is about the relationship between the mechanical analysis and permeation measurements. Thanks to its processability properties, and its flexibility and high elongation modulus, LLDPE was selected to be used for packaging and storing food. Therefore, the study of gas diffusion properties is of great interest, particularly the characterization of oxygen, carbon dioxide, methane, ethane, ethylene, propane, and propylene, which is the goal of this article.

Preceding studies¹⁰ using these kind of semi crystalline polyethylene were focused on the role played by the inter phase effect between amorphous and crystalline boundaries, which decreases the Henry solubility¹¹ constant and the diffusion coefficient.³ Therefore, assuming a modified free volume with an impermeable-crystalline component in the material (semi crystalline-free volume model), it can help to explain the variation of the solubility coefficient.^{12,13} But it remains to analyze the changes on P and D with temperature and concentration.

In this article, we proceed to show that by means of the use of the dual-semicrystalline model it is possible to explain the variation of the gas diffusion for oxygen, carbon dioxide, methane, ethane, ethylene, propane and propylene, using LLDPE as a function of density or crystalline percentage, at temperatures of 25 and 35 °C. The results for the diffusion coefficient, and the permeability parameter for the gases tested have been interpreted assuming that the amorphous part of the polymer represents a continuum phase in which Henry's sites are homogeneously distributed, whose volume fraction decreases when the crystalline fraction increases.

On the other hand, increasing the percentage of crystallinity, the microcavities or Langmuir sites increases, so that the Langmuir sites in semicrystalline LLDPE play a more important role than the Henry's sites.¹⁴ However, the last produce the tortuosity in the gas trajectory and chain immobilization increase in the amorphous phase, therefore, the diffusion coefficient is diminished. The result shows that its dependence with the crystallinity fraction follows an exponential rule, as it will be discussed later.

Finally, the thermodynamic counterparts of the tortuosity and chain immobilization factors will be discussed.

EXPERIMENTAL

Films Preparation

Polyethylene supplied by Dow (Tarragona, Spain), specifically, Dowlex 2740 E, Dowlex 2045 E, Attane SC-4108, and Engage 8200, whose commercial densities are 0.940, 0.920, 0.904, and 0.870 g/cm³, respectively, were used. LDPE films were prepared by compression molding between two heating plates at 200 °C for 15 min. Then the films were cooled at room temperature. The acronyms for the films in decreasing order of crystallinity are, PE94, PE92, PE90, and PE87, respectively.

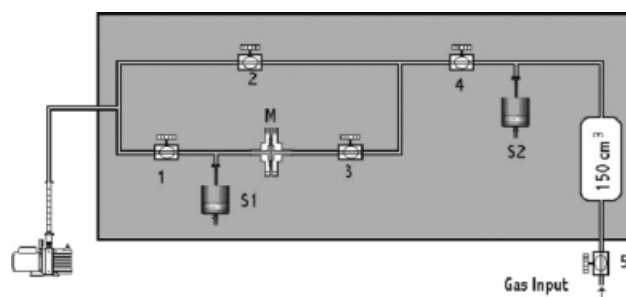


FIGURE 1 Experimental device used in the gas permeability measurements. M: membrane. S1 and S2 pressure sensors. 1, 2, 3, 4, and 5 electrovalves.

Permeation Measurements

Permeation measurements of oxygen, carbon dioxide, methane, ethane, ethylene, propane, and propylene in the films were carried out in the experimental device schematically represented in Figure 1. The apparatus consists of two chambers, separated by the membrane, immersed in a thermostatic bath controlled by a computer. Vacuum is made in the two chambers by means of a Leybold AG vacuum pump model Trivac D 1,6 B that can reach 4×10^{-4} mbar. Pressures are measured using capacitive sensors. Leybold DI 2000 sensor (S1) and Tylan General CDHD45-11 sensor (S2), with an accuracy of 0.15% of reading, were used in the upstream- and downstream chambers, respectively. Nupro pneumatic valves model SS-4BK-1C controlled from a computer using electrovalves were utilized. A computer program controls temperature, vacuum, gas filling of the upstream chamber, measurement of pressures in the chambers, and calculates both permeability and diffusion coefficients. The program automatically repeats this job for each temperature and pressure of the upstream chamber. Before each series of measurements, the system was vacuum calibrated by measuring the inlet of air into the downstream chamber. Keeping all the valves open but valve 5 closed, high vacuum was made for 24 h in both chambers. Then valves 2 and 3 were closed, and valve 5 was opened thus allowing the gas to fill a 150 cc deposit at a pressure close to that of the experiment. The program computer suddenly closed valve 1 and opened valve 3 taking as zero this time. The evolution of the pressure in the downstream chamber with time was monitored with the transducer pressure sensor CDHD45-11. The permeation measurements were performed at the temperature constant of 25 °C.

The permeability coefficient P , was obtained from the slope of the straight line of the p versus t plot by means of the expression

$$P = 3.59 \frac{VL}{p_0 AT} \lim_{t \rightarrow \infty} \left\{ \frac{d[p(t)]}{dt} \right\} \quad (1)$$

where $p(t)$ and p_0 are, respectively, the pressure in the downstream and upstream chambers in cmHg, V is the volume of the downstream chamber in cm³, A is the area of the membrane in cm², L is the thickness of the sample in cm,

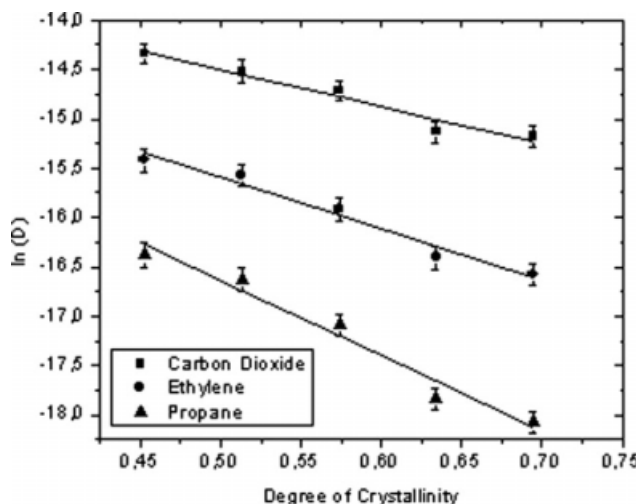


FIGURE 2 Natural logarithm of D versus de degree of crystallinity, for carbon dioxide, ethylene and propane.

and T , the absolute temperature. Using these units, P is given in barrers [1 barrer = 10^{-10} cm³(STp) cm/(cm² s cmHg)]. The diffusion coefficient was obtained by the time-lag method, that corresponds to the intersection of the straight line p versus t with the abscissa axis, using the equation suggested by Barrer¹⁵

$$D = \frac{L^2}{6\theta} \tag{2}$$

where θ is the time lag.

The relative error Δ , involved in the determination of the diffusion coefficient by the time-lag method was obtained by the following expression

$$\Delta = \frac{100}{D} \left[\frac{L\varepsilon(L)}{3\theta} + \frac{L^2\varepsilon(\theta)}{6\theta^2} \right] \tag{3}$$

where $\varepsilon(L)$ and $\varepsilon(\theta)$ are the errors involved in the evaluation of the thickness of the films and the time-lag, respectively. It should be pointed out that even in the most unfavorable case; the error estimated in the determination of the apparent diffusion coefficient in semicrystalline LLDPE films was lower than 10%.

The precision of the permeability coefficient $\varepsilon(m)$, was estimated from the slope $m = dp/dt$ of the isotherm in the steady state conditions, and the correlation coefficient of the straight line r , according to the expression.

$$\varepsilon(m) = m \frac{\tan(\arccos(r))}{\sqrt{N-2}} \tag{4}$$

where N is the number of experimental points used in the straight line determination. The precision obtained for the permeability were about 2–3% for all gases in all the films studied.

Diffusion Coefficient Results

We assume the following expression for the diffusion coefficient in terms of the crystalline fraction and temperature:

$$D(\alpha_{\text{cris}}, T) = D^*(T) \exp(-A(T) \cdot \alpha_{\text{cris}}) \tag{5}$$

where $D^*(T)$ is the diffusion coefficient of the gas in completely amorphous polymer matrix, $A(T)$ is a constant quantity independently of the presence of crystalline phase and α_{cris} is the phase crystalline fraction. The plot of the logarithm of the diffusion coefficient in terms of the crystalline fraction for carbon dioxide, ethylene, and propane at 25 °C, is given in the Figure 2. The crystalline fraction was determined from density data by using the prescription given in reference.¹⁶ The fitting values for several gases are reported in the Table 1.

Thermodynamic Interpretation of the Diffusion Coefficient Expression for a Semicrystalline Polymer

In the homogeneous membrane model, the gas-filled space through which transport of permeates can occur may be conceived as fluctuating pores or channels of the polymeric matrix, which are not fixed either in size nor in location. As a consequence of the fluctuating effect, the free volume in a polymer membrane exhibits a fair degree of mobility so that the size and the shape of the pores or channels may continuously change. The geometry of the polymer network sets upper limit for the size of such pores and also for the size of the molecules which can permeate. The transport is dependent on the probability that the permeate molecules find a hole at their locations. Therefore, considering that diffusion is a thermal activated process, the diffusion coefficient can be expressed as

$$D = \nu \exp\left(-\frac{\Delta G^{++}}{RT}\right) \tag{6}$$

where ν is the translational oscillation frequency of the diffusing molecule; it is related to the diffusion jump distance λ and Boltzmann's and Planck's constants by $\nu \approx \lambda^2(kT/h)$, and has the units cm²/s. The quantity ΔG^{++} is the activation free energy for the diffusion process.

In the case of semicrystalline polymers ΔG^{++} is dependent on three parameters (α_{am}, T, p), where α_{am} is the amorphous phase fraction. Under isothermal and isobaric conditions, according to the previous view of gas diffusion in a semicrystalline polymer, the variation of the total Gibbs free

TABLE 1 Slope and $\ln D^*$ Values From $\ln D$ versus Degree of Crystallinity Plot, Reported for Several Gases

Gas	$\ln(D^*)$	A (slope)
Oxygen	-13.103	-1.7461
Carbon Dioxide	-12.602	-3.7905
Methane	-12.729	-4.5519
Ethane	-12.867	-6.1479
Ethylene	-12.985	-5.219
Propane	-12.826	-7.6288
Propylene	-12.713	-6.7853

TABLE 2 Slope and $\ln D^*$ Values From $\ln D$ versus Degree of Crystallinity Plot, Reported for Several Gases by Michaels (1964)¹⁹

Gas	$\ln(D^*)$	A (slope)
Oxygen	-13.095	-3.1551
Carbon Dioxide	-13.385	-3.1347
Methane	-13.743	-3.7118
Ethane	-14.46	-4.4828
Ethylene	-	-
Propane	-15.036	-5.0685
Propylene	-14.657	-4.5689

energy is only given by taking into account the amorphous phase, and is only dependent of α_{am} .

So that, $\Delta G^{++} = \alpha_{\text{am}} \Delta G_{\text{am}}^{++}$ where $\Delta G_{\text{am}}^{++} = \Delta G_{\text{am}}^{++} (\alpha_{\text{am}} = 1, T)$, and then

$$D(\alpha_{\text{am}}, T) = v \exp\left(-\frac{\alpha_{\text{am}} \Delta G_{\text{am}}^{++}}{RT}\right) \quad (7)$$

For the case of polymer as amorphous pure phase, eq 7 becomes

$$D^*(T) = v \exp\left(-\frac{\Delta G_{\text{am}}^{++}}{RT}\right) \quad (8)$$

The ratio for diffusion coefficient of eqs 7 and 8 is the following

$$\frac{D^*(T)}{D(\alpha_{\text{am}}, T)} = \exp\left(-\frac{\Delta G_{\text{am}}^{++}}{RT} (1 - \alpha_{\text{am}})\right) = \exp(A\alpha_{\text{crys}}) \quad (9)$$

where we have used that $\alpha_{\text{am}} + \alpha_{\text{crys}} = 1$.

From eq 9, the formal expression for the parameter A can be established

$$A = -\frac{\Delta G_{\text{am}}^{++}}{RT} \quad (10)$$

where $\Delta G_{\text{am}}^{++}$ is the activation free energy for gas diffusion in the amorphous part of the polymeric matrix.

Comparison with Michael and Bixler

In the previous work of Peterlin,¹⁷ Gedde and coworker,¹⁸ Michael and Parker,¹⁰ and Michael and Bixler,¹⁹ the ratio of the diffusion coefficients between the amorphous phase and the semicrystalline one, is expressed by

$$\frac{D^*(T)}{D(\alpha_{\text{am}}, T)} = \beta\tau \quad (11)$$

where τ is the tortuosity factor, and β is the immobilization factor, accounted for restricted segmental mobility of amorphous chains near the amorphous-crystalline interphase, due to the crosslinking-type effect of crystallites.

TABLE 3 Comparison of Expressions $\ln(\beta) + \ln(\tau)$ and $(A\alpha_{\text{crys}})$ for Ethane. Here $n = 1.88$ and $n = 1.25$

α_{crys}	$\ln(\beta) + \ln(\tau)$	$A\alpha_{\text{crys}}$	$A\alpha_{\text{crys}}$ (Michaels)
$n = 1.88$			
0.77	7.162990824	4.733883	4.303761
0.43	2.806783566	2.643597	2.403399
0.29	1.793881781	1.782891	1.620897
$n = 1.25$			
0.77	6.237094963	4.733883	4.303761
0.43	2.452648648	2.643597	2.403399
0.29	1.578112886	1.782891	1.620897

Now, we are interested to analyze their proposal in terms of the result of eq 9, so we concern on the logarithm relationship which results from eqs 9 and 11, that is,

$$\ln(\beta) + \ln(\tau) = A\alpha_{\text{crys}} \quad (12)$$

Data in Tables 2–7 show a behavior, which is the same found in data reported by Michaels and Bixler (ref. 20). for the gases oxygen, carbon dioxide, methane, ethane, and propane.

From the comparison of the Michaels and Bixler data with ours in Tables 2–6, we reach the same conclusions proposed in eq 5, concerning to the dependence of the diffusion coefficient on α_{crys} .

Diffusion Coefficient Analysis

Thermodynamic Interpretation of the Parameter τ and β

The diffusion coefficient can be expressed as²⁰

$$D = v \exp\left(-\frac{\Delta \bar{G}^{++}}{RT}\right) = v \exp\left(-\frac{\Delta \bar{H}^{++}}{RT}\right) \exp\left(\frac{\Delta \bar{S}^{++}}{R}\right) \quad (13)$$

The quantities $\Delta \bar{G}^{++}$, $\Delta \bar{H}^{++}$, and $\Delta \bar{S}^{++}$ are the free energy of activation, the enthalpy of activation for the diffusion processes, and entropy of activation, respectively.

We now consider the diffusion coefficient for a pure amorphous membrane.

TABLE 4 Comparison of Expressions $\ln(\beta) + \ln(\tau)$ and $(A\alpha_{\text{crys}})$ for Methane. Here $n = 1.88$ and $n = 1.25$

α_{crys}	$\ln(\beta) + \ln(\tau)$	$A\alpha_{\text{crys}}$	$A\alpha_{\text{crys}}$ (Michaels)
$n = 1.88$			
0.77	5.162990824	3.504963	3.449831
0.43	2.256783566	1.957317	1.926529
0.29	1.743881781	1.320051	1.299287
$n = 1.25$			
0.77	4.237094963	3.504963	3.449831
0.43	1.902648648	1.957317	1.926529
0.29	1.528112886	1.320051	1.299287

TABLE 5 Comparison of Expressions $\ln(\beta) + \ln(\tau)$ and $(A\alpha_{\text{crys}})$ for Oxygen. Here $n = 1.88$ and $n = 1.25$

α_{crys}	$\ln(\beta) + \ln(\tau)$	$A\alpha_{\text{crys}}$	$A\alpha_{\text{crys}}$ (Michaels)
$n = 1.88$			
0.77	4.462990824	1.344497	2.971199
0.43	2.356783566	0.750823	1.659241
0.29	1.643881781	0.506369	1.119023
$n = 1.25$			
0.77	3.537094963	1.344497	2.971199
0.43	2.002648648	0.750823	1.659241
0.29	1.428112886	0.506369	1.119023

$$D_{\text{am}} = v \exp\left(-\frac{\Delta\bar{G}_{\text{am}}^{++}}{RT}\right) = v \exp\left(-\frac{\Delta\bar{H}_{\text{am}}^{++}}{RT}\right) \exp\left(\frac{\Delta\bar{S}_{\text{am}}^{++}}{R}\right) \quad (14)$$

here the quantities $\Delta\bar{G}_{\text{am}}^{++}$, $\Delta\bar{H}_{\text{am}}^{++}$, and $\Delta\bar{S}_{\text{am}}^{++} = 0$ are the free energy, enthalpy of activation for the diffusion processes, and entropy of activation, respectively, for the case of 100% amorphous membrane.

The ratio of the diffusion coefficients of the amorphous phase and the semicrystalline one, using eqs 13 and 14, is the following

$$\frac{D^*(T)}{D(\alpha, T)} = \exp\left(-\frac{\Delta G_D}{RT}\right) = \exp\left(-\frac{\Delta H_D}{RT}\right) \exp\left(-\frac{\Delta\bar{S}^{++}}{R}\right) \quad (15)$$

where $\Delta G_D = \Delta\bar{G}_{\text{am}}^{++} - \Delta\bar{G}^{++}(T, \alpha)$, $\Delta H_D = \Delta\bar{H}_{\text{am}}^{++} - \Delta\bar{H}^{++}(T, \alpha)$.

From eq 15 we identify the product $\beta\tau$, as it was given by eq 11, then

$$\beta = \exp\left(-\frac{\Delta H_D}{RT}\right) \quad (16)$$

$$\tau = \exp\left(\frac{\Delta\bar{S}^{++}}{R}\right) \quad (17)$$

Interpretation of the Tortuosity Factor

The tortuosity factor is physically interpreted in terms of the change of the activation entropy induced by the

TABLE 6 Comparison of Expressions $\ln(\beta) + \ln(\tau)$ and $(A\alpha_{\text{crys}})$ for Propane. Here $n = 1.88$ and $n = 1.25$

α_{crys}	$\ln(\beta) + \ln(\tau)$	$A\alpha_{\text{crys}}$	$A\alpha_{\text{crys}}$ (Michaels)
$n = 1.88$			
0.77	9.262990824	5.874176	4.969349
0.43	3.056783566	3.280384	2.775091
0.29	1.813881781	2.212352	1.871573
$n = 1.25$			
0.77	8.337094963	5.874176	4.969349
0.43	2.702648648	3.280384	2.775091
0.29	1.598112886	2.212352	1.871573

TABLE 7 Comparison of Expressions $\ln(\beta) + \ln(\tau)$ and $(A\alpha_{\text{crys}})$ for Carbon dioxide. Here $n = 1.88$ and $n = 1.25$

α_{crys}	$\ln(\beta) + \ln(\tau)$	$A\alpha_{\text{crys}}$	$A\alpha_{\text{crys}}$ (Michaels)
$n = 1.88$			
0.77	4.462990824	2.918685	3.065447
0.43	2.106783566	1.629915	1.711873
$n = 1.25$			
0.77	3.537094963	2.918685	3.065447
0.43	1.752648648	1.629915	1.711873

presence of the crystalline phase, as it will be seen in the time being.

The concept of the activation entropy is related to the additional difficulties for the diffusion particle in the activated state to go from one site to another. That is, the required entropy change represents the hindrances in the diffusion path when the crystalline phase is present.

That can be explained in another way.

Consider that the activation entropy can be expressed in terms of the number of conformations in which one trajectory of the heterogeneous phase can bifurcate (Ω^{++}) when the crystalline phase is present. $\Delta S_D = kT \ln \Omega^{++}$. Therefore $\tau = \Omega^{++}$.

Now the diffusion coefficient depends on the conformation number, and can be written as

$$D(\alpha_{\text{am}}, T) = \frac{v}{\Omega^{++}} \exp\left(-\frac{\Delta\bar{H}^{++}}{RT}\right) \quad (18)$$

Since there is not contribution of the activation entropy for a homogeneous phase, we have for the purely amorphous phase $\Omega^{++} = 1$, and $\tau = 1$; $\Delta S_D = 0$, that corresponds to the 100% amorphous matrix. Taking this value as reference, the diffusion process requires increase in the activation entropy when the crystalline fraction increases.

Therefore, in this interpretation the tortuosity factor is related to the number of new conformations raised by the hindrances present in the path diffusion. Along these terms the activation entropy is related to the heterogeneous degree in the composed phase.²¹

To quantify the conformation number or the activation entropy, one can see the change in the intersection of the ordinates axis in an Arrhenius plot.

The Problem of the Tortuosity Factor Formulation

Peterlin (ref. 17) Michaels and Bixler (ref. 19) determined the tortuosity factor for a series of PEs, and they have given the following expression to describe the experimental data.

$$\ln \tau = -n \ln(1 - \alpha_{\text{crys}}), \quad (19)$$

They report two values for the parameter n depending on the polymerization preparation. For Ziegler catalysts and

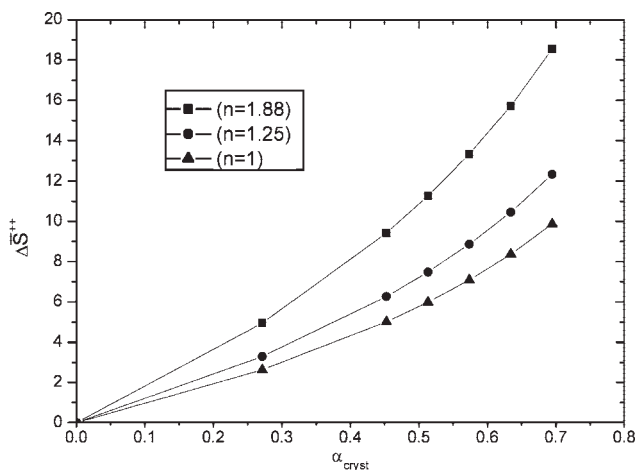


FIGURE 3 $\Delta\bar{S}^{++}$ versus α_{crys} for three values of n . The curves are independent of the gas.

branched and linear high pressure polyethylene $n = 1.88$. For Philips catalysts and hydrogenated polybutadienes $n = 1.25$. The increase of n is related to the spherical morphology of the crystals and the type of the polymeric network.²² The dependence of n takes into account the changes of the interphase crystal-polymer randomly distributes and the nature of the polymeric matrix.

Taken the logarithm of the tortuosity factor from eqs 17 and 19, it is possible to identify the activation entropy change

$$\Delta\bar{S}^{++} = -n \cdot R \cdot \ln(1 - \alpha_{\text{crys}}) \quad (20)$$

In Figure 3 it can be seen that the activation entropy increases when the crystalline fraction does. The slop of this curve depends on the value of n .

On the other hand, for nonspherulitic crystals another variable has to be introduced to describe in a complete form the tortuosity factor; $X = w/l$. Where w is the width and l is the thickness of the crystals. According to H. Fricke²³ slight modifications of X results in an appreciable variation in the tortuosity factor.

Another effect to be included in the activation entropy is the crystal orientation of nonspherulitic crystals, present when the heterogenous nucleation is developed. Related to this effect, the anysotropic diffusion has been reported.²⁴⁻²⁶ Up to day, an unified formulation of tortuosity factor, taking into account the crystal morphology, heterogenous nucleation, interphase crystal-polymer effect, as well the crystallization degree is an incomplete task.

Interpretation of the Immobilization Factor

The identification of the immobilization β , in eq 16, involves the activation enthalpy given by $\Delta\bar{H}^{++} = E_D + RT$, where E_D is the activation energy, that is, it is the energy required to open a cylindrical cavity of diameter equal to that of the permanent molecule d , and with a length λ , in a medium of cohesive density energy E_{CED} . Accordingly²⁷

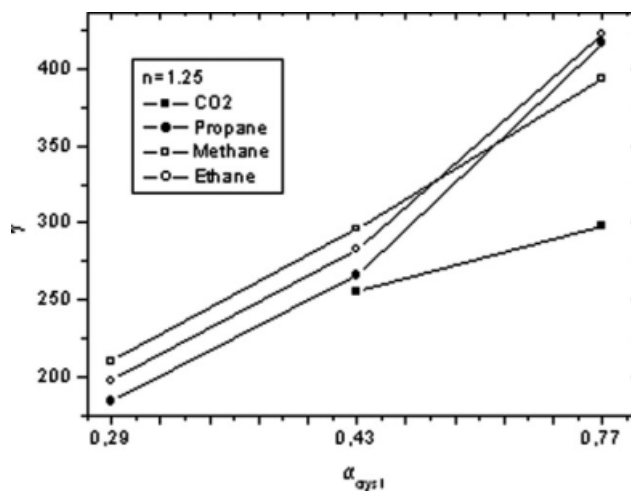


FIGURE 4 γ versus α_{crys} for several gases. Parameter $n = 1.25$.

$$E_D = \frac{\pi}{4} d^2 \lambda N_A E_{\text{CED}} \quad (21)$$

where N_A is the Avogadro's number. The change of the enthalpy activation can be modeled using the change of the cohesive energy density

$$\Delta E_{\text{CED}} = E_{\text{CED}} - (E_{\text{CED}})_{\text{am}} \quad (22)$$

then,

$$\Delta H_D = -\frac{\pi}{4} \lambda d^2 N_A \Delta E_{\text{CED}} = \gamma d^2 \quad (23)$$

where d^2 is the reduced molecular diameter squared in angstrom,² and λ is the characteristic jump distance. The parameter γ is the second parameter of Michaels and Bixler, and is equal to

$$\gamma = -\frac{\pi}{4} \lambda N_A \Delta E_{\text{CED}}. \quad (24)$$

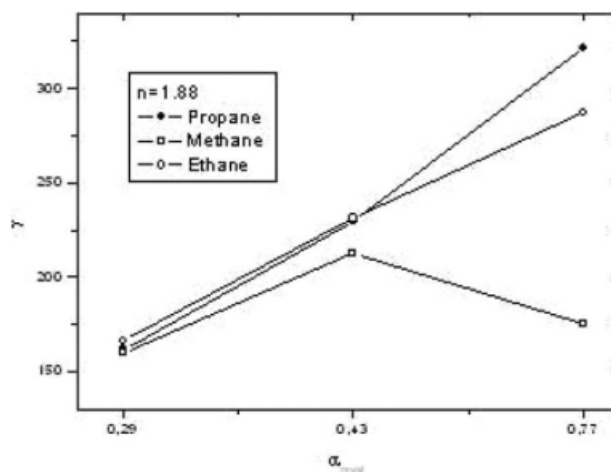


FIGURE 5 γ versus α_{crys} for several gases. Parameter $n = 1.88$.

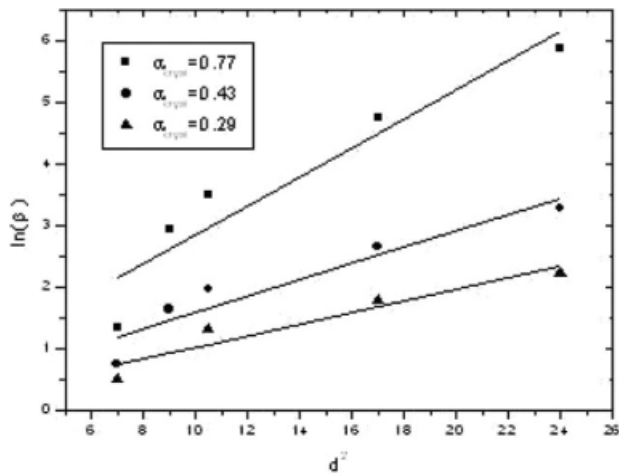


FIGURE 6 $\ln \beta = \frac{\gamma}{RT} d^2$ versus reduced molecular diameter squared d^2 (angstrom²).

Therefore, the immobilization chain factor is given in terms of this parameter

$$\beta = \exp\left(\frac{\gamma d^2}{RT}\right) \quad (25)$$

The physical interpretation of the factor β is established by means of eq 25. That is, an increment in crystallinity increases the cohesive energy density, and so does immobilization of the polymeric chains.

Now, using eqs 12, 18, and 25, we are able to obtain one expression for the parameter γ .

$$\gamma = \frac{RT}{d^2} [A\alpha_{crys} + n \ln \alpha_{am}] \quad (26)$$

In Figures 4 and 5, it is shown the obtained values for the parameter γ in terms of the crystalline fraction.

Along these terms, we conclude that the immobilization factor increases due to the increase on the cohesive energy, related in turn to the increasing of the Langmuir center or crystalline portion.

In Figure 6, it is shown the dependence of $\ln \beta = \frac{\gamma}{RT} d^2$ on the reduced molecular diameter squared.²⁸ This plot shows the particular nature of the parameter γ , as it is proposed here.

Finally, it should be stressed that the parameters n and γ depends on the thermal history and the polymerization mode²⁹ on the sample, which introduce a new variable, and it does make any approach incomplete. However, it is possible to predict the gas diffusivity and permeability on the basis of the level of crystallinity, if the analysis is based using polyethylene samples produced by similar conditions of thermal history and polymerization. This is the case presented in our approach.

Free Volume Model Interpretation of the Chain Immobilization Factor

For a semicrystalline polymer through which diffusion occurs in the amorphous component, it is possible to identify the

enthalpy contribution to the gas diffusion in terms of the free volume. Accordingly to the Gedde and coworkers,³⁰ it has for the enthalpy contribution in eq 16 the following relationship

$$\frac{\Delta H}{RT} = \frac{B_d \phi_A (f_1 - f_2)}{f_2 (f_2 + \phi_A (f_1 - f_2))} \quad (27)$$

where the fractional free volume of the gas penetrate is (f_1), the fractional free volume of the amorphous fraction of the pure polymer is (f_2). Naturally, the polymer free volume (f_2) diminishes as a consequence of the increasing of the crystalline fraction. ϕ_A is the volume fraction of the gas and ϕ_P is the volume fraction of the polymer. $\phi_A + \phi_P = 1$. B_d is a constant depending on the geometry of the molecular gas.

In obtaining eq 27, it was supposing that the gas penetrating brings free volume to the amorphous fraction. In this complementary view of the interpretation of the activation enthalpy and ultimately of the immobilization chain factor, it depends on the difference in the free volume of gas and polymer matrix, and on the concentration of the gas in the membrane, as it was pointed out by Peterlin (ref. 11).

Permeability Analysis

To analyze the permeability, we consider the expressions given for diffusion in eq 9, and the following expression for the solubility.

$$S = \alpha_{am} S_{am} \quad (28)$$

The permeability have been considering given according to

$$P = D \cdot S \quad (29)$$

therefore

$$P = \alpha_{am} P^* e^{-A\alpha_{crys}} \quad (30)$$

where

$$P^* = D^* \cdot S_{am} \quad (31)$$

In Figure 7, it is shown the dependence of the permeability on the crystalline fraction for several gases using eq 30 and comparing to the experimental values. The agreement between these values is enough to conclude that the validity of eq 29 prevails for semicrystalline polymers, where the diffusion coefficient and sorption dependence have their main dependence on the crystalline fraction.

CONCLUSIONS

The dual-semicrystalline model describes the sorption, diffusion coefficient and permeability constant behavior of LLPD depending on temperature and crystalline fraction. It is based in the following assumptions:

1. There are two phases in the material, the polymeric matrix and the dispersed one. The former is an amorphous phase and the last one is given by small crystal regions.

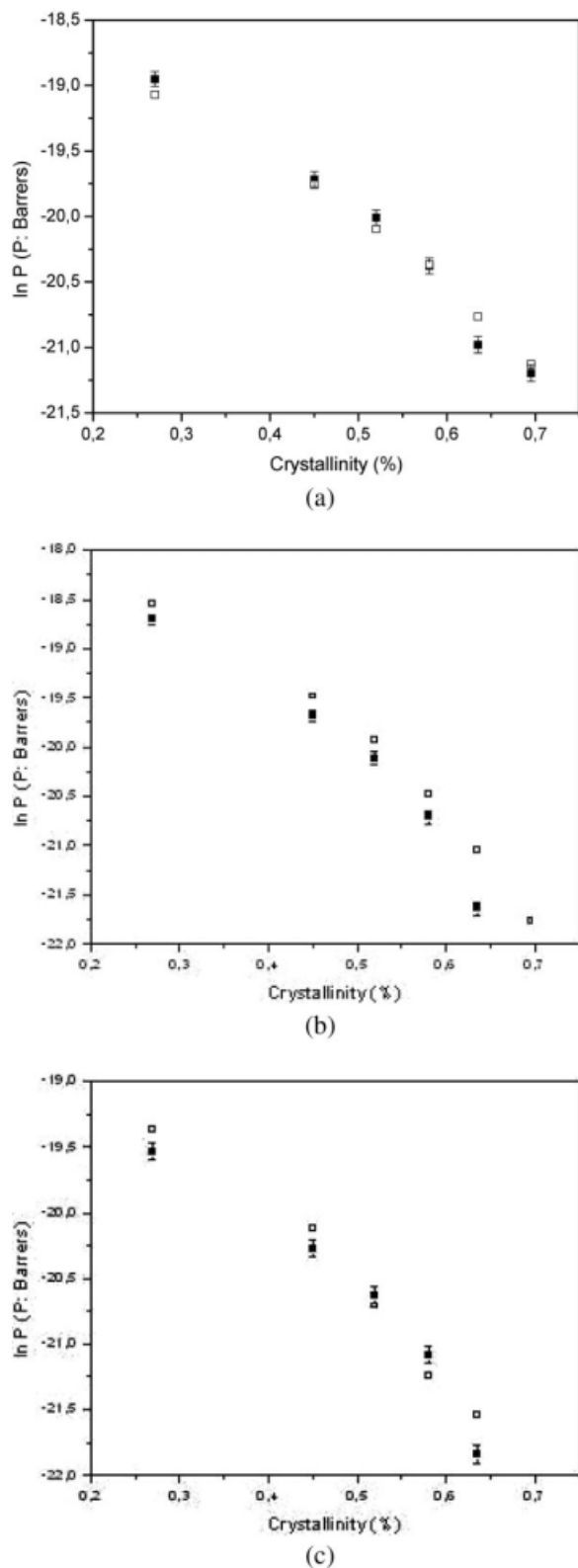


FIGURE 7 Natural permeability versus the Degree of crystallinity, for: (a) Carbon dioxide, (b) Propane and (c) Ethylene. Black squares are experimental data and the open squares correspond to theory (eq. 29).

The original polymeric matrix is modified by the inter-phase polymer-crystal, which becomes important when the crystal fraction increases.

2. The amorphous phase is where the gas sorption and diffusion takes place.
3. The decreasing of the diffusion coefficient is explained in terms of the effect of the crystalline phase on the polymeric phase. In fact, the modification of the amorphous phase is explained by the two following factors: (1) the tortuosity and (2) the chain immobilization, as it was proposed by Michaels and Parker (refs. 2 and 3), and Michaels and Bixler (ref. 12). Both factors increase when the crystalline fraction increases.
4. In terms of the results of this work, both parameters have a thermodynamic interpretation, as it was shown in the text. The tortuosity factor is related to the increases of the activation entropy ΔS^{++} , which could be modeled by $\Delta S^{++} = -nR \ln \alpha_{am}$, where n is a parameter depending on the material.

Regarding to the chain immobilization factor, it is related to the change of cohesive energy density, produced by the crosslinking effect of the crystallites on the amorphous phase. The consequence of this is that the dependence of diffusion coefficient on the reduced molecular diameter squared is introduced through the change of the activation energy, according to eq 23.

The resulting expression for the diffusion coefficient is given by

$$D(\alpha_{am}, T) = D_0 \exp\left(-\frac{(E_D)_{app}}{RT}\right) \quad (32)$$

where

$$D_0 = v \exp\left(\frac{\Delta S_D}{R}\right) \quad (33)$$

And the apparent activation energy $(E_D)_{app}$ is given by the sum of two contributions, one corresponding to the amorphous part and one corresponding to the change induced by the crystalline phase.

$$(E_D)_{app} = (E_D)_{am} + \gamma d^2 \quad (34)$$

So far, in the resulting model there are two fitting parameters, one is $(E_D)_{am}$ and the other is the constant n . The parameter γ can be obtained from eq 26.

This work was supported by the Dirección General de Investigación Científica y Técnica (DGICYT), Grant MAT-2005-05648-C02-01, Instituto de la Pequeña y Mediana Industria Valenciana (IMPIVA), Grant IMCOVA-2006/20, and DGAPA-UNAM Proyecto IN 112109, and proyecto IMPULSA-UNAM (PUNTA).

REFERENCES AND NOTES

- 1 Forni, C. Brite- Euram -BE Project 4104; Brussels, 1995.
- 2 Michaels, A. S.; Bixler, H. J Polym Sci 1961, 50, 393.

- 3** Michaels, A. S.; Bixler, H. J. *J Polym Sci* 1959, 41, 33.
- 4** Ohya, H.; Kudryavtsev, V. V.; Semenova, S. I.; *Polyimide Membranes*; Gordon and Breach Publishers: Tokyo, 1996.
- 5** Koros, W. J.; Fleming, G. K. *J Memb Sci* 1993, 83, 1.
- 6** Stern, S. A. *J Memb Sci* 1994, 94, 1.
- 7** Al-Masri, M.; Kricheldorf, H. R.; Fritsch, D. *Macromolecules* 1999, 32, 7853.
- 8** Petropoulos, J. H. *Pure Appl Chem* 1993, 65, 219.
- 9** Compañ, V.; Ribes, A. Diaz-Calleja, R.; Riande, R. *Polymer* 1995, 36, 323.
- 10** (a) Koros, W. J.; Paul, D. R.; Rocha, A. A. *J Polym Sci: Polym Phys Ed* 1976, 14, 687; (b) Tsujita Y. *Chinese J Poly Sci* 2000, 18, 301; (c) Osada, T.; Nakagawa, T. In *Membrane Science and Technology*, Marcel-Dekker Inc, 1992; p 3–58.
- 11** Jeschke, D.; Stuart, H. A. *Z Naturforsch* 1961, 16a, 37; (b) Michaels, A. S., Bixler, H. J., Fein, H. L. *J Appl Phys* 1964, 35, 3165.
- 12** Compañ, V.; López, M. L.; Andrio, A.; Riande, A. *Macromolecules* 1998, 31, 6984.
- 13** Compañ, V.; Andrio, A. López, M. L.; Riande, E. *Polymer* 1996, 37, 5831.
- 14** Compañ, V.; del Castillo, L. F.; Hernández, S. I.; López, M. L.; Riande, E. *J Polym Sci Part B: Polym Phys* 2007, 45, 1798.
- 15** Barrer, R. M. *Trans Faraday Soc* 1939, 35, 628.
- 16** Balta Calleja, F. J.; Rueda, D. R. *Polym J* 1974, 6, 216.
- 17** Peterlin, A. *J Macromol Sci Phys* 1975, B11, 57.
- 18** Hedenqvist, M.; Angelstok, A.; Larsson, P. T.; Gedde, U. W. *Polymer* 1966, 37, 2887.
- 19** Michaels, A. S.; Bixler, H. J. *J Polym Sci* 1961, 50, 413.
- 20** Glasstone, S.; Laidler, K. J.; Eyring, H. *The Theory of Rate Process*, McGraw-Hill: New York, 1941.
- 21** Sing, A.; Koros, W. J. *Ind Eng Chem Res* 1996, 35, 1231.
- 22** Hedenqvist, M.; Gedde, U. W. *Prog Polym Sci* 1996, 21, 299.
- 23** Hamilton, R. L.; Crosser, O. K. *Ind Eng Chem Fundam* 1962, 3, 187.
- 24** Barrer, R. M.; Petropoulos, J. H. *Brit J Appl Phys* 1961, 12, 691.
- 25** Takagi, Y. *J Appl Polym Sci* 1965, 9, 3887.
- 26** Prevorsec, D. C., Marget, P. J., Sharma, R. K. *J Macromol Sci Phys* 1974, B8, 127.
- 27** Kumins, C. A.; Kwei, T. K. In *Diffusion in Polymers*, Crank, J.; Park, G. S., Eds.; Academic Press: New York, 1968; Chapter 4.
- 28** Puelo, A. C.; Paul, D. R.; Wong, P. K. *Polymer* 1989, 30, 1357.
- 29** Czernico, J.; Baddour, R. F.; Cohen, R. E. *Macromol* 1987, 20, 2468.
- 30** Neway, B.; Hedenqvist, M. S.; Mathot, V. B. F.; Gedde, U. W. *Polymer* 2001, 42, 5307.